

Absence of Criticality in the Phase Transitions of Open Floquet Systems

Steven Mathey* and Sebastian Diehl

Institut für Theoretische Physik, Universität zu Köln, 50937 Cologne, Germany

(Dated: August 19, 2022)

Floquet systems hold the promise to realize novel phases of matter without equilibrium counterpart. The coupling to a bath can stabilize a stationary state at finite energy density. We address here the nature of phase transitions in such systems at rapid drive, complementary to the Kibble-Zurek scenario at slow drive. While the infinitely rapidly driven limit exhibits a second order phase transition, here we reveal a universal mechanism showing that fluctuations associated to the first rotating wave correction drive the transition first order at any finite driving. The effect is rooted in the degeneracy of critical poles in weakly coupled higher Floquet-Brillouin zones, in some analogy to the Coleman-Weinberg or Halperin-Lubensky-Ma phenomenon. The critical exponents of the infinitely rapidly driven fixed point – including a new, independent one – can be probed experimentally upon smoothly tuning towards that limit.

Introduction – Many-body Floquet systems [1, 2] – ensembles of particles subject to periodic driving – have recently triggered enormous research interest, both in experiments and from a theoretical perspective. For example, very rapid drive can lead to effective conservative dynamics on short enough time scales, as was successfully exploited for Hamiltonian engineering of artificial gauge fields for ultracold atoms [3, 4]. When instead the driving frequency Ω is closer to the natural energy scales of the problem, phenomena directly tied to driving can be observed, such as time crystals in atomic [5, 6] and ionic [7] systems. Theoretical research spans the question of equilibration [8–13], the search for novel topological states without equilibrium counterparts [14–18], or driven analogs of many-body localization [19–21].

Specifically when it comes to implementations of periodically driven quantum systems with generic interactions, the ensuing irreversibility can lead to unbounded heating [8–10, 22–25]. This represents an important hurdle to experimental implementation of many of the anticipated phenomena. A natural cure is to couple the driven system to a bath, such that the system can reach a finite entropy Floquet steady state, with observables synchronized to the drive. Often such baths occur quite naturally, such as phonons in solid state superfluids [26–30]. Further examples include quantum dots and optical cavities [31–35], Brownian motors [36–38], spin chains [6, 22, 39, 40] or cold atoms in optical lattices [41].

A natural and fundamental question in this large class of periodically driven, open quantum systems concerns the effect of the periodic drive on symmetry breaking phase transitions. Previous work has addressed this question in the slowly driven limit, establishing the connection to Kibble-Zurek physics [42–44], as well as intermediate driving frequencies [6, 45–47]. The effect of fast, but not infinitely fast driving remained elusive so far. In this work, we focus on a minimal model for a weakly and rapidly periodically driven open quantum system

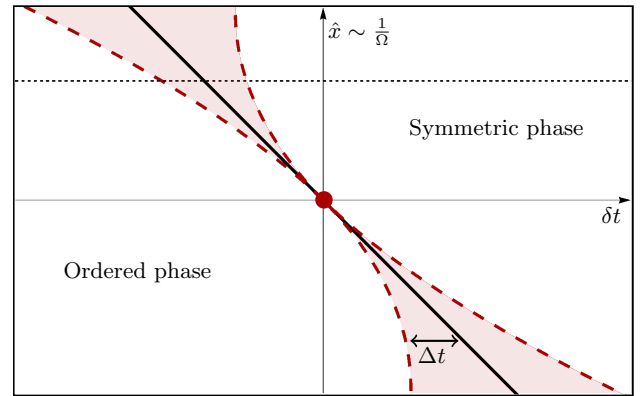


FIG. 1. Schematic phase diagram of the open Floquet Bose system in three dimensions. δt is the distance from the phase transition in the infinitely rapidly driven system, $\hat{x} \sim \Omega^{-1}$ is the rescaled drive coefficient [cf. Eq. (7)]. The symmetry breaking phase transition occurs at the solid black line. It is second order only at $\Omega^{-1} = 0$ (red dot). Otherwise, fluctuations associated to the periodic drive transform the phase transition to weakly first order. The dashed red lines represent a crossover region between the known $\Omega^{-1} = 0$ scaling regime and one where scaling is frozen out (light red). The black dotted line represents a typical experimental path through the phase diagram.

with phase rotation symmetry in three dimensions (3d). We identify a universal mechanism, according to which a seeming second order phase transition is unavoidably driven first order by fluctuations.

Basic physical picture – At first sight, the qualitative modification of the critical behavior by a fast scale may appear counterintuitive. It can be rationalized, however, when taking into account the fact that energy is not conserved in open Floquet systems. It is only defined modulo Ω , representing the possibility of exchanging energy quanta $n\Omega$ with the driving field – a notion of ‘high’ and ‘low’ energies, or ‘slow’ and ‘fast’ modes, is thus not well defined *a priori*.

Let us first consider the undriven situation for an open

* smathey@thp.uni-koeln.de

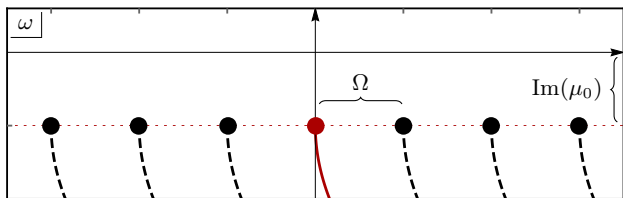


FIG. 2. Location of the poles of the retarded Green function. The absence of energy conservation gives rise to arbitrarily many poles spaced by Ω .

system. The poles of the single-particle Green functions are then located on a line, whose real part can be adjusted to zero by a choice of rotating frame (central solid line in Fig. 2). Criticality is achieved when the line reaches the real axis, i.e. when the slowest damping rate approaches zero. A Renormalisation Group (RG) program is then well-defined, and implemented by integrating out those modes first, which are farthest away from the real axis.

This situation is drastically different for a periodically driven open system: As a consequence of the Floquet formalism, poles are located not only on one central line, but also on all Floquet copies of that line spaced by Ω (dashed lines in Fig. 2). These correspond to the different Floquet-Brillouin zones (FBZ). In particular, when the problem becomes critical, all lines extend jointly towards the real axis. In consequence, the usual strategy of integrating out modes to find the effective low energy theory has to be carefully adapted: Within each of the lines of poles, RG can be performed in the standard way; but in principle, all the critical poles associated to different lines have to be taken into account. We find, however, that with increasing distance from the central one (that remains for $\Omega^{-1} = 0$), the poles are parametrically suppressed for a weak and fast drive. We take advantage of this in the present work and devise an expansion in powers of Ω^{-1} . In addition, we work at 1-loop order, which is systematic to first order in powers of $\epsilon = 4 - d$. The approach presented below is a double expansion, and systematic at $\mathcal{O}(\Omega^{-1}) \times \mathcal{O}(\epsilon)$.

The fact that phase transitions can be driven from second to first order by virtue of strong fluctuations occurs also in other contexts. One class is provided by the Coleman-Weinberg or Halperin-Lubensky-Ma mechanism, where additional gapless modes – such as gauge fields [48, 49] or Goldstone modes [50, 51] – compete with the critical ones in the vicinity of a phase transition. A second class derives from the Potts model, where the common prerequisite is that a continuous *external* (order parameter) symmetry is explicitly broken down to a non-trivial discrete subgroup (e.g. $U(1) \rightarrow Z_3$ in the Potts model [52, 53], or similar phenomena in $O(N)$ models [54, 55]). This allows for new operators that may turn out to be relevant. Here we reveal a third class, where a continuous *internal* symmetry (time translation invariance) is broken down to a discrete one – while keeping

the external phase rotation symmetry $U(1) \simeq O(2)$ fully intact. Since discrete time translation invariance and energy conservation modulo Ω are two sides of the same coin, this provides an alternative, RG based viewpoint on our mechanism.

Open Floquet dynamics – Microscopically, our system is made of generic interacting particles on a lattice, governed by a Hamiltonian with a bounded energy spectrum, and coupled to an external bath. The periodic time-dependence typically occurs in the Hamiltonian $H(t + 2\pi/\Omega) = H(t)$, but it could also enter through periodic excitations of the bath. The dynamics be equipped with a $U(1)$ phase rotation symmetry, which is also respected by the drive. Our focus will be on phase transitions in $3d$ systems, where the phase rotation symmetry can be broken spontaneously. Close to the transition, larger scale fluctuations dominate the physics, and we can employ an effective semiclassical, mesoscopic Landau-Ginzburg-type model for the complex order parameter ϕ to describe the driven open dynamics in terms of a Langevin equation,

$$i\partial_t \phi = [K\nabla^2 - \mu - g|\phi|^2] \phi + \xi. \quad (1)$$

ξ is a Gaussian white noise, which has correlation $\langle \xi(t, \mathbf{x}) \xi^*(t', \mathbf{x}') \rangle = 2\gamma \delta(t - t') \delta(\mathbf{x} - \mathbf{x}')$, with $\gamma > 0$, and vanishes on average. The couplings K, μ, g are complex valued. Their real parts account for the coherent dynamics inherited from the underlying Hamiltonian, and the imaginary parts of μ and g have an interpretation as incoherent one- and two-body sources and sinks of particles resulting from the coupling to the bath [56, 57]. These imaginary parts determine the phase structure of the system's stationary state. In particular, a second order phase transition accompanied with the spontaneous breakdown of phase rotation symmetry occurs in the undriven system when $\text{Im}(\mu)$ is lowered below its critical value. In our case, all couplings are time-dependent with period $2\pi/\Omega$ in the Floquet steady state, as a consequence of the microscopic drive. For definiteness, we choose a monochromatic drive

$$\begin{aligned} \mu &= \mu_0 + \mu_1 e^{i\Omega t} + \mu_{-1} e^{-i\Omega t}, \\ g &= g_0 + g_1 e^{i\Omega t} + g_{-1} e^{-i\Omega t}. \end{aligned} \quad (2)$$

Not only in the undriven limit $\mu_{\pm 1} = g_{\pm 1} = 0$, but also in the limit of infinitely fast driving $\Omega \rightarrow \infty$, an effectively time-independent, yet driven-dissipative model emerges. The latter limit is appropriate for typical settings in quantum optics, or quantum optical many-body systems [56–58]. In that case, in the rotating wave approximation, the driving scale is approximated as infinitely fast $\Omega^{-1} = 0$. This problem exhibits a true second order phase transition, but a modified criticality compared to equilibrium due to the microscopic breaking of detailed balance [59, 60].

Here we focus on weakly and rapidly driven Floquet systems, where the driving frequency Ω is large, but still of comparable order to the other energy scales of the

problem. Technically, we incorporate the leading rotating wave corrections $\mathcal{O}(\Omega^{-1})$ into the analysis of the near-critical driven open many-body problem.

Action and symmetries – We re-write the stochastic dynamics of Eq. (1) in terms of a dynamical functional integral [57, 61], using the effective action $\Gamma[\Phi]$,

$$e^{i\Gamma[\Phi]} = \int D\varphi e^{i(S[\Phi+\varphi] + \int_{t,\mathbf{x}} \varphi \delta\Gamma[\Phi]/\delta\Phi)}, \quad (3)$$

which includes all the field fluctuations, and provides the correlation and response functions. Eq. (1) translates to the mesoscopic action

$$S = \int_{t,\mathbf{x}} \Phi^\dagger \begin{pmatrix} 0 & G_A^{-1} \\ G_R^{-1} & P_K \end{pmatrix} \Phi + (g \tilde{\phi}^* \phi |\phi|^2 + \text{c.c.}), \quad (4)$$

with $G_R^{-1} = i\partial_t - K\nabla^2 + \mu$, $G_A^{-1} = i\partial_t - K^*\nabla^2 + \mu^*$ and $P_K = i\gamma$. $\Phi = (\phi, \tilde{\phi})$ contains the order parameter ϕ , as well as the ‘response’ or ‘quantum’ field $\tilde{\phi}$ that is inherent to the dynamical functional formalism. The following symmetry considerations will guide our understanding:

(i) Discrete time translations: Continuous time translations are implemented by $\Phi(t) \rightarrow \Phi(t + \Delta t)$ for arbitrary Δt . A monochromatic drive with frequency Ω , breaks this continuous symmetry down to a discrete one, under $\Phi(t) \rightarrow \Phi(t + 2\pi n/\Omega)$, n integer. The continuous symmetry is restored in the undriven limit $\mu_{\pm 1} = g_{\pm 1} = 0$ [see Eq. (2)], but also in the infinitely rapidly driven limit $\Omega^{-1} = 0$, where the rotating wave approximation is applicable. Conversely, its explicit breaking allows for the presence of additional dimensionful couplings $\mu_{\pm 1}$ and $g_{\pm 1}$. These are not compatible with the undriven dynamical ϕ^4 theory, and will lead to a new relevant direction at the Wilson-Fisher (WF) fixed point.

(ii) Absence of detailed balance: Thermodynamic equilibrium can be formulated in terms of a dynamical symmetry, whose presence is equivalent to the obedience of thermal fluctuation-dissipation relations, i.e. detailed balance [62–64]. Out of equilibrium, this symmetry is generically lost because the system is exposed to different drives and baths, preventing thermalization. It can then formally be recovered by fine tuning. In our case, this would amount to having the ratios of all pairs of complex couplings to be both real and time independent (see Sect. C). Whenever this unnatural fine tuning is not realized, we will encounter the effect described in this work. In this sense, it is generic, or universal, for periodically driven, open quantum systems.

Single-particle Green functions and critical poles – In the Wigner representation [10, 65–68] the single-particle Green functions $G_n(\omega)$, are the double Fourier transform of the Green functions in the time domain $G(t, t')$ (See Sect. A1). The discrete time-translation invariance is encoded in the discrete index n . We obtain an explicit expression for the retarded Wigner Green function $G_{R;n}(\omega)$, in Sect. A2, which demonstrates that $G_{R;n}(\omega)$ is composed of an infinite sum of poles located on lines in the complex plane (see Fig. 2). The residues of the poles

of $G_{R;n}(\omega)$ are organised in a power series in $\mu_{\pm 1}/\Omega$. This means that a systematic expansion of the loop corrections in powers of Ω^{-1} is obtained by expanding the Green functions in powers of $\mu_{\pm 1}/\Omega$ before the frequency integrations are performed. To order 1 in $\mu_{\pm 1}/\Omega$, we find

$$G_{R;0}(\omega, \mathbf{q}) = h_0^R(\omega, \mathbf{q}), \quad h_0^R(\omega, \mathbf{q}) = (\omega + K\mathbf{q}^2 + \mu_0)^{-1},$$

$$G_{R;n \neq 0}(\omega, \mathbf{q}) = -\mu_n h_0^R(\omega - \frac{n\Omega}{2}, \mathbf{q}) h_0^R(\omega + \frac{n\Omega}{2}, \mathbf{q}). \quad (5)$$

$h_0^R(\omega, \mathbf{q})$ describes the fundamental pole in the single-particle Green functions. We emphasize that this expansion still captures the correct pole structure and their location, which is fixed by the Floquet formalism. We see that the Green functions involve poles separated by integer multiples of Ω , that all become critical as $\text{Im}\mu_0 \rightarrow 0$.

Perturbation theory – As anticipated above, care must be taken when renormalizing the problem, due to the absence of a direct meaning of ‘high’ and ‘low’ energies. More practically, this forces us to keep the various poles on equal footing. This imposes another summation index in the diagrammatics, over the FBZ label n . The point is illustrated in the one-loop correction to the self-energy at zero frequency and momentum,

$$\Delta\mu_0 = 2i \sum_n \int_{\omega, \mathbf{q}} g_n G_{K;-n}(\omega, \mathbf{q}). \quad (6)$$

Using $G_K = -G_R P_K G_A$ and inserting the expansion (5), we can perform the frequency integral and expand it to $\mathcal{O}(\Omega^{-1})$ to obtain

$$\Delta\mu_0 = \gamma \int_{\mathbf{q}} \frac{1}{|\text{Im}(K\mathbf{q}^2 + \mu_0)|} (g_0 + ix),$$

$$x = \frac{i}{\Omega} \sum_{n \neq 0} \frac{g_{-n} (\mu_n - \mu_{-n}^*)}{n} \equiv \sum_{n \neq 0} \tilde{g}_n. \quad (7)$$

This shows explicitly the appearance of divergences from the $n = 0$ term, describing processes exclusively within the zeroth FBZ, but also from $n \neq 0$, which describe scattering between different FBZs enabled by the drive. Along the frequency integral of Eq. (6), each pole contributes with the same degree of divergence. For a monochromatic drive however, find $\text{Res}(\omega_n) \sim (\mu_{\pm 1}/\Omega)^n$, which leads to a suppression of terms involving higher FBZs. Thus, all the FBZs contribute to the critical physics through these divergences, but interactions between different FBZs are parametrically small in μ_n/Ω .

Renormalization group analysis – Equipped with the understanding of parametrically small but equally divergent contributions from the coupling to higher FBZs at leading order in $1/\Omega$, we proceed to the resummation of these divergences in an RG analysis to study its impact on the critical behavior. We first fix the canonical power counting: We transform spatial and temporal coordinates under scale transformations as $\hat{\mathbf{q}} = \mathbf{q}/k$ and $\hat{\omega} = \omega/(\text{Im}(K)k^2)$. The couplings are then rescaled as

$$\hat{\mu}_n = k^{-2} \frac{\mu_n}{\text{Im}(K)}, \quad \hat{g}_n = k^{d-4} \frac{\gamma g_n}{4\text{Im}(K)^2}. \quad (8)$$

To keep the argument of the oscillatory function dimensionless, we also have to rescale $\hat{\Omega} = \Omega/(\text{Im}(K)k^2)$. This defines the canonical scaling at the Gaussian fixed point (with \tilde{g}_n being rescaled as g_n).

In order to assess the relevance of these couplings at the interacting WF fixed point established at $\Omega^{-1} = 0$ [60], we include fluctuations into our RG analysis. To this end, we work at leading order in the $\epsilon = 4 - d$ expansion, where the fluctuation analysis is controlled at one-loop order. The RG flow equations for μ and g take the form of a coupled set of differential equations for the dependence of the Fourier modes μ_n and g_n , on the running cut-off scale k (see Sect. B). To order Ω^{-1} , the RG flow equations of $\hat{\mu}_0$ and \hat{g}_0 are

$$\begin{aligned} k\partial_k \hat{g}_0 &= -\epsilon \hat{g}_0 + \frac{10S_d}{|1 + \hat{\mu}_0|(1 + \hat{\mu}_0)} \hat{g}_0 \left(\hat{g}_0 + \sum_m \hat{g}_{m \neq 0} \right), \\ k\partial_k \hat{\mu}_0 &= -2\hat{\mu}_0 - \frac{4S_d}{|1 + \hat{\mu}_0|} \left(\hat{g}_0 + \sum_{m \neq 0} \hat{g}_m \right), \end{aligned} \quad (9)$$

with $S_d = 2\pi^{d/2}/[(d/2 - 1)!(2\pi)^d]$. The drive parameter is $\hat{x} = \sum_m \hat{g}_m$. Here and in the following we have simplified our system to make the computation more transparent: We discard a time dependence of γ and K , which does not lead to modifications of the scenario (cf. Sect. D). Furthermore, we choose K , μ and g to be purely imaginary. Physically, this anticipates the decoherence that occurs in the vicinity of the phase transition, where all coherent dynamics fades away under coarse graining [60]. We have extracted a factor i from μ_0 , g_0 and K . The couplings were renamed as $\mu_0 = i\mu'_0$, $g_0 = ig'_0$ and $K = iK'$ with μ'_0 , g'_0 and K' real. We omit the primes to simplify the notation.

In principle, additional variables must be taken into account to compute the RG flow of \hat{x} , since it depends on all the harmonics of μ and g (See Eq. (7)). However, as we show in the Sect. B, the loop corrections to the flow of x can be neglected at $\mathcal{O}(\Omega^{-1}) \times \mathcal{O}(\epsilon)$, giving rise to simple dimensional running according to

$$k\partial_k \hat{x} = -\epsilon \hat{x}. \quad (10)$$

The RG flow equations (9) and (10) provide a generalisation of the well known, time translation invariant, RG flow. Indeed, the WF fixed point emerges when $\hat{x} = 0$. Our analysis reveals that the periodic drive gives rise to a new relevant coupling. In the absence of continuous time translation invariance, the critical point is thus bi-critical: Two fine tunings are necessary to reach it, and to reveal its critical scaling properties. In the absence of drive and far away from the critical point, the system is either in a disordered or an ordered phase. This property is robust for a finite, rapid drive since the Green functions are gapped in these phases (cf. Fig. 2), and perturbation theory converges [69]. Thus, when tuning across the symmetry breaking phase transition at finite Ω^{-1} (along the dotted line of Fig. 1) the additional relevant direction provides a finite correlation length scale.

This gives rise to a symmetry breaking phase transition without asymptotic criticality, which must be interpreted as a fluctuation induced first order phase transition.

The linear stability analysis of the RG flow equations close to the WF fixed point provides three quantitative predictions:

(i) New scaling exponent: We find three critical exponents: $-2 + 2\epsilon/5 = -1/\nu$, ϵ and a new independent exponent $-\epsilon = -1/\nu_d$. The first two are known, with the first being negative and corresponding to the relevant direction. When the system is infinitely rapidly driven, it is tuned to criticality via $\delta\mu = \hat{\mu}_0 - \mu_0^*$ and $\delta g = \hat{g}_0 - g_0^*$ through $\delta t \sim (\delta g + 4\pi^2 \delta\mu)$, and the correlation length diverges as $\xi \sim \delta t^{-\nu}$. In the presence of a drive however ($\hat{x} \neq 0$), the correlation length never diverges. δt can be tuned to maximize it (or, in RG terms, bring the flow as close as possible to the WF fixed point), but ξ always saturates to a finite value that scales as $\xi \sim \hat{x}^{-\nu_d}$.

(ii) Shift of the phase transition: To each critical exponent corresponds an eigenvector of the stability matrix. See Sect. F for explicit expressions. The two negative critical exponents (or eigenvalues) correspond to the two relevant directions. The new relevant direction is not perpendicular to the two others, and generic initial conditions for the RG flow are given by

$$(\delta\mu, \delta g, \hat{x}) = \frac{\epsilon(\delta t + A\hat{x})}{5A} \vec{v}_1 + \left[\delta g + \frac{\hat{x}}{2} \left(1 + \frac{\epsilon}{5} \right) \right] \vec{v}_2 + \hat{x} \vec{v}_3,$$

with $\delta t = A(\delta g + 4\pi^2 \delta\mu)$, $A > 0$ a non-universal constant, and $\vec{v}_{1,3}$ are the two relevant directions. This equation shows that a finite value of \hat{x} shifts the location of the phase transition, Fig. 1.

(iii) Observability of scaling: In the presence of the drive, the location of the phase transition is then defined as $\Delta t = \delta t + A\hat{x} = 0$. For $\Delta t > 0$, the system is in the symmetric phase; the $O(2)$ symmetry is broken for $\Delta t < 0$. The above scaling analysis can be refined by replacing δt by Δt , because \hat{x} and Δt control the crossover between the two scaling regimes. For $|\Delta t| \gg |\hat{x}|^{\nu_d/\nu}$, the undriven relevant coupling dominates and the correlation length scales as $\xi \sim \Delta t^{-\nu}$. When $|\Delta t| \ll |\hat{x}|^{\nu_d/\nu}$ the correlation length saturates to $\xi \sim \hat{x}^{-\nu_d}$. This crossover is represented as red dashed lines in Fig. 1. The correlation length scales with Δt outside of the light red area and it saturates as the dashed red lines are crossed. In particular, this implies that the new critical exponent ν_d can be observed by varying Ω .

Conclusion – We close by pointing out an interesting 'duality' of our scenario to the paradigmatic Kibble-Zurek phenomenology [70, 71]. Both the equilibrium limit of an undriven system $\Omega = 0$, and the infinitely rapidly driven limit $\Omega^{-1} = 0$, afford time-independent descriptions, and exhibit symmetry breaking continuous phase transitions. Here we have shown that the leading correction $\mathcal{O}(\Omega^{-1})$ universally transforms phase transitions in Floquet driven open quantum systems from second to first order, in this way cutting off asymptotic scal-

ing at any finite Ω^{-1} . Conversely, the Kibble-Zurek phenomenon occurs in the opposite limit of a slow driving: The leading correction from driving necessarily leads to a breakdown of adiabaticity near the phase transition, which universally leads to the freeze-out of dynamics via the production of defects. Although the underlying mechanisms are very different, in both cases the critical physics is masked and observable only upon smoothly approaching the extreme limiting cases. Exploring the connection between these phenomena deserves further scrutiny.

Another intriguing direction of research concerns the applicability of our results to possible phase transitions in long-lived transient states of Floquet systems not coupled to external baths, before their ultimate approach to the infinite temperature state [72].

Acknowledgments - We thank A. Altland, C.-E. Bardyn, M. Buchhold, A. Gambassi, M. Heyl, A. Lazarides, G. Loza, J. Marino, R. Moessner, F. Piazza, A. Polkovnikov, G. Refael, A. Rosch, D. Roscher, M. Scherer, K. Seetharam, U. Täuber and J. Wilson for useful and inspiring discussions. We acknowledge support by the Institutional Strategy of the University of Cologne within the German Excellence Initiative (ZUK 81) and the European Research Council via ERC Grant Agreement n. 647434 (DOQS).

Appendix A: Green functions

In this section we discuss the Green functions in the Floquet steady state. In Sect. A 1 we define the Wigner and Floquet Green functions and show how they are computed in general. In Sect. A 2 we compute analytically the single-particle retarded Green function and elucidate its pole structure.

1. Definitions

We exploit here the fact that physical observables are periodic in their center of mass time in the synchronized Floquet steady state. The Green functions

$$G(t, t') = -i \begin{pmatrix} \langle \phi(t) \phi^*(t') \rangle & \langle \phi(t) \tilde{\phi}^*(t') \rangle \\ \langle \tilde{\phi}(t) \phi^*(t') \rangle & \langle \tilde{\phi}(t) \tilde{\phi}^*(t') \rangle \end{pmatrix}, \quad (\text{A1})$$

take the following form,

$$G(t, t') = \sum_n \int_{\omega, \mathbf{q}} e^{-i[\omega(t-t') - \mathbf{q} \cdot \mathbf{r} + n\Omega(t+t')/2]} G_n(\omega, \mathbf{q}).$$

$\mathbf{r} = \mathbf{x} - \mathbf{x}'$ denotes the relative spatial coordinate, which we do not write explicitly on the left-hand-side. $G(t, t')$ is a periodic function of $t_a = (t + t')/2$ and can be represented in terms of the Wigner Green functions [10, 65–

68],

$$G_n(\omega, \mathbf{q}) = \int_{\tau, \mathbf{r}} \int_{t_a} e^{i[\omega\tau - \mathbf{q} \cdot \mathbf{r} + n\Omega t_a]} G(t_a + \tau/2, t_a - \tau/2), \quad (\text{A2})$$

which encode the time periodicity with a discrete index. Here and in the following, we use the short-hand notation $\int_{\omega, \mathbf{q}} = 1/(2\pi)^{d+1} \int_{-\infty}^{\infty} d\omega \int_{-\infty}^{\infty} d^d q$, $\int_{\tau, \mathbf{r}} = \int_{-\infty}^{\infty} d\tau \int_{-\infty}^{\infty} d^d r$ and $\int_{t_a} = \Omega/(2\pi) \int_0^{2\pi/\Omega} dt_a$. Furthermore, the Floquet Green functions are defined as,

$$G_{nm}(\omega) = G_{n-m} \left[\omega + (n+m) \frac{\Omega}{2} \right], \quad |\omega| \leq \frac{\Omega}{2}, \quad (\text{A3})$$

which are two-index Green functions constructed from the single index Wigner Green functions.

These definitions are directly applicable to the inverse Green functions, G^{-1} . Specifically, $G^{-1}(t, t')$ is [see Eq. (4) of the main text]

$$G^{-1}(t, t') = \begin{pmatrix} 0 & i\partial_t - K^* \nabla^2 + \mu^* \\ i\partial_t - K \nabla^2 + \mu & i\gamma \end{pmatrix} \delta(t - t'),$$

and $G_{nm}^{-1}(\omega)$ reads

$$G_{nm}^{-1}(\omega) = \begin{pmatrix} 0 & G_{A;nm}^{-1}(\omega) \\ G_{R;nm}^{-1}(\omega) & P_{K;nm}(\omega) \end{pmatrix}, \quad (\text{A4})$$

with

$$\begin{aligned} G_{R;nm}^{-1} &= \delta_{nm} (\omega + n\Omega) + K_{n-m} p^2 + \mu_{n-m} \\ &= \delta_{nm} (\omega + n\Omega + M_0) + \delta_{nm+1} \mu_1 + \delta_{nm-1} \mu_{-1}, \\ G_{A;nm}^{-1} &= \delta_{nm} (\omega + n\Omega) + K_{n-m}^* p^2 + (\mu_{m-n}^*) \\ &= \delta_{nm} (\omega + n\Omega + M_0^*) + \delta_{nm+1} \mu_{-1}^* + \delta_{nm-1} \mu_1^*, \\ P_{K;nm} &= i\gamma_{n-m} = i\delta_{nm} \gamma. \end{aligned} \quad (\text{A5})$$

μ_n is the n -th Fourier mode of μ . The expressions after the second equalities are specific to a monochromatic drive with frequency Ω and K and γ constant, and $M_0 = Kp^2 + \mu_0$.

The Floquet Green functions are introduced because they provide an efficient means to compute the Green functions from G^{-1} . Indeed, G is computed from the inverse Green functions through

$$G(t, t') = \begin{pmatrix} -[G_R P_K G_A](t, t') & G_R(t, t') \\ G_A(t, t') & 0 \end{pmatrix}, \quad (\text{A6})$$

and G_X (with $X = R$ or A) is defined as the functional inverse of G_X^{-1} , $\int_{\tau} G_X^{-1}(t, \tau) G_X(\tau, t') = \delta(t - t')$. The products that appears in the top-left entry of Eq. (A6) are also functional, $AB(t, t') = \int_{\tau} A(t, \tau) B(\tau, t')$. The Floquet representation of the Green functions (A3), has the advantage that it turns functional inverses into matrix inverses. In other words, the following statements are equivalent,

$$\begin{aligned} \int_{\tau} G(t, \tau) G^{-1}(\tau, t') &= \delta(t - t'), \\ \sum_s G_{ns}(\omega) G_{sm}^{-1}(\omega) &= \delta_{nm}. \end{aligned} \quad (\text{A7})$$

2. Poles

In this section we compute $G_{R;n}(\omega, \mathbf{q})$ analytically and show that it has an infinite number of poles with identical imaginary parts and real parts separated by integer multiples of Ω . The main result of this section is Eq. (A13) with the additional constraint that, in the sum, only terms where m has the same parity as n contribute. For definiteness, we work with a monochromatic drive, Eq. (2) of the main text.

We start by computing the single-particle retarded Green function in real time, $G_R(t, t') = -i\langle\phi(t)\tilde{\phi}^*(t')\rangle$. Without interaction, the solution of Eq. (1) of the main text is

$$\phi(t) = \phi(t_0)e^{i\int_{t_0}^t M(t')dt'} - i\int_{t_0}^t e^{i\int_{t'}^t M(t'')dt''}\xi(t')dt', \quad (\text{A8})$$

with $M(t) = Kp^2 + \mu(t)$ the real time representation of the right-hand-side of the single-particle equation of motion ($M_0 = Kp^2 + \mu_0$ and $M_{n\neq 0} = \mu_n$). We now exploit the following relation

$$G_R(t, t') = \frac{\delta\langle\phi(t)\rangle_f}{\delta f(t')}\Big|_{f=0}, \quad (\text{A9})$$

where $\langle\dots\rangle_f$ is the average over a modified noise $\xi' = \xi + f$. This noise has the same Gaussian statistics and variance as ξ , but it does not average to zero. Instead we have $\langle\xi'(t)\rangle_f = f(t)$. Then, the average of Eq. (A8) is

$$\langle\phi(t)\rangle_f = \langle\phi(t_0)\rangle_f e^{i\int_{t_0}^t M(t')dt'} - i\int_{t_0}^t e^{i\int_{t'}^t M(t'')dt''}f(t')dt',$$

and we obtain

$$G_R(t, t') = -i\theta(t - t')e^{i\int_{t'}^t M(t'')dt''}. \quad (\text{A10})$$

In the Floquet steady state, $t_0 \rightarrow -\infty$ and the term containing t_0 is negligible because $\text{Im}(M_0) > 0$.

We now partially convert $G_R(t, t')$ to its Wigner form

$$G_R(\omega, t_a) = \int_{\tau} e^{i\omega\tau} G_R(t_a + \tau/2, t_a - \tau/2). \quad (\text{A11})$$

To this end, we write

$$G_R(t_a + \tau/2, t_a - \tau/2) = -i\theta(\tau)e^{iM_0\tau} \text{Exp}\left[\frac{2i\sin\left(\frac{\Omega\tau}{2}\right)}{\Omega}(M_1e^{i\Omega t_a} + M_{-1}e^{-i\Omega t_a})\right],$$

and use $e^{iz\sin(\theta)} = \sum_m J_m(z)e^{im\theta}$ (Jacobi-Anger expansion), with $J_m(x)$ the m -th Bessel function of the first kind,

$$G_R(t_a + \tau/2, t_a - \tau/2) = -i\theta(\tau)e^{iM_0\tau} \sum_m J_m\left[\frac{2(M_1e^{i\Omega t_a} + M_{-1}e^{-i\Omega t_a})}{\Omega}\right] e^{i\Omega m\frac{\tau}{2}}.$$

Finally we obtain

$$G_R(\omega, t_a) = \sum_m \frac{J_m\left[\frac{2(M_1e^{i\Omega t_a} + M_{-1}e^{-i\Omega t_a})}{\Omega}\right]}{\omega + M_0 + \frac{m\Omega}{2}}. \quad (\text{A12})$$

From the above equation, it appears that the poles are spaced by half-integer multiples of Ω . This is however not the case because only half of the terms of the above sum contribute to the Wigner Green function $G_{R;n}(\omega) = \int_{t_a} e^{in\Omega t_a} G_R(\omega, t_a)$. To see this, we expand the Bessel function and look at the Fourier transform of each term,

$$G_{R;n}(\omega) = \sum_{s=0}^{\infty} \frac{(-1)^s \Omega^{-2s}}{s!} \left[\frac{H_{n,0,s}}{s!(\omega + M_0)} + \sum_{m=1}^{\infty} \frac{\Omega^{-m}}{(s+m)!} \left(\frac{H_{n,m,s}}{\omega + M_0 + \frac{m\Omega}{2}} + \frac{(-1)^m H_{n,m,s}}{\omega + M_0 - \frac{m\Omega}{2}} \right) \right], \quad (\text{A13})$$

with

$$H_{n,m,s} = \int_{t_a} e^{in\Omega t_a} (M_1e^{i\Omega t_a} + M_{-1}e^{-i\Omega t_a})^{2s+m} = \sum_{r=0}^{2s+m} \binom{2s+m}{r} M_1^{2s+m-r} M_{-1}^r \delta_{2s-2r+m+n}.$$

The Fourier transform produces a constraint that can only be satisfied if $n + m$ is even. Then n and m must have the same parity and half of the terms in the sum of Eq. (A13) vanish.

Eq. (A13) provides an exact expression for the single-particle Green function. Although it is not really useful for practical calculations, it elucidates the analytical structure of the Wigner Green functions. This is most clearly seen in Eq. (A12): The frequency dependence of the single-particle Green function is composed of an infinite sum of poles that all have the same imaginary parts and are spaced by integer multiples of Ω . Moreover, the residues of each pole are analytical functions of $M_{\pm 1}/\Omega$. Then, expanding $G_{n;R}$ to order 1 in $M_{\pm 1}/\Omega$ provides

$$G_{R;n}(\omega) = \frac{\delta_{n0}}{\omega + M_0} - \frac{M_n(1 - \delta_{n0})}{(\omega + M_0)^2 - \left(\frac{\Omega}{2}\right)^2}, \quad (\text{A14})$$

which, recalling that $M_0 = Kq^2 + \mu_0$ and $M_{n\neq 0} = \mu_{n\neq 0}$, is Eq. (5) of the main text.

Appendix B: RG flow equations

In this section we show how to obtain RG flow equations including loop corrections for all the Fourier modes of μ and g . Although we expand the RG flow equations to order Ω^{-1} , this approach can be applied to include higher order corrections. We recover Eqs. (9) and (10) of the main text.

The RG flow equations of μ and g are similar to the undriven case although with additional sums over the Fourier indexes and propagators that are modified by the periodicity of μ . To 1-loop order (and for arbitrary Ω), the RG flow equations of μ_n and g_n take the form

$$\begin{aligned}
k\partial_k g_n &= 2iS_d k^d \sum_{\substack{m_1, m_2 \\ m_3, m_4}} g_{m_4} \delta_{n, m_1 1234} \int_{\omega} \\
&\times \left\{ G_{R; m_1}(\omega, k) G_{K; m_2} \left[-\omega - \frac{m_3 - m_4}{2} \Omega, k \right] g_{m_3} \right. \\
&+ 2G_{A; m_1}(\omega, k) G_{K; m_2} \left[\omega - \frac{m_4 - m_3}{2} \Omega, k \right] (g_{-m_3})^* \\
&\left. + 2G_{R; m_1}(\omega, k) G_{K; m_2} \left[\omega - \frac{m_3 - m_4}{2} \Omega, k \right] g_{m_3} \right\}, \\
k\partial_k \mu_n &= -2iS_d k^d \sum_m \int_{\omega} g_m G_{K; n-m}(\omega, k); \quad (\text{B1})
\end{aligned}$$

$m_{1234} = \sum_{i=1}^4 m_i$ and $S_d = 2\pi^{d/2} / [(d/2 - 1)!(2\pi)^d]$. Both equations are obtained by integrating out 1-loop fluctuations within a momentum shell $k - dk < p < k$ and taking the limit $dk \rightarrow 0$. $G_{K; n}$, $G_{R; n}$ and $G_{A; n}$ are the Wigner Green functions, which are defined in Eq. (A2), and g_n are the Fourier modes of g . The above equations do not contain any approximation in the Floquet sector. The complexity of the Floquet formalism is hidden in the Wigner Green functions.

We emphasize that the full frequency integral is unavoidable here. The sharp momentum cut-off (inherent to momentum-shell renormalization) fixes the loop momentum to $p = k$ and the frequency integrals are performed by closing the integral path in the complex plane and using the residue theorem. As we discuss in the main text, the poles of the Green functions are located along a line in the complex plane with identical imaginary parts and real parts separated by integer multiples of the drive frequency, $\omega_n = -Kk^2 - \mu_0 + n\Omega$. See Sect. A2. In usual RG approaches, there is only one pole (with $n = 0$). Then, the frequency axis is effectively cut-off since only frequencies with $\omega \sim k^2$ contribute to the loop integrals. Only small energies contribute. Although, this is technically very similar to our problem (find the poles and use residue theorem), it is physically very different. Indeed, Floquet formalism forces us to consider all the poles on equal footing and there is no cut-off on the frequency axis.

We now discuss how the RG flow equations Eq. (B1), can be simplified in the presence of a weak and fast drive. This expansion is carried out in three steps: (i) The Wigner Green functions are expanded in powers of $\mu_{n \neq 0}$ up to a given order. See e.g. Eq. (A14), where $G_{R; n}(\omega)$ is expanded to order 1. This provides a simplified set of Green functions that are inserted in the RG flow equations [Eq. (B1)]. (ii) The frequency integrals are performed analytically with the residue theorem. (iii) The obtained expressions are expanded in powers of Ω^{-1} up

to the same order as the $\mu_{n \neq 0}$ expansion of step (i).

To order Ω^{-1} , the RG flow equations are

$$\begin{aligned}
k\partial_k \mu_n &= -\frac{S_d k^d \gamma}{|\text{Im}(M_0)|} (g_n + iX_n), \\
k\partial_k g_{2r+1} &= \frac{S_d k^d \gamma}{|\text{Im}(M_0)|} Y_{2r+1}, \\
k\partial_k g_{2r} &= \frac{S_d k^d \gamma}{|\text{Im}(M_0)|} \\
&\times \left\{ \left[\frac{g_r}{2M_0} + \frac{g_r - (g_{-r})^*}{i\text{Im}(M_0)} \right] (g_r + iX_r) + Y_{2r} \right\}. \quad (\text{B2})
\end{aligned}$$

Here and in the following we use $M_0 = Kk^2 + \mu_0$. Y_n and X_n provide $\mathcal{O}(\Omega^{-1})$ corrections

$$\begin{aligned}
X_n &= \frac{i}{\Omega} \sum_{m \neq 0} \frac{g_{n-m} (\mu_m - \mu_{-m}^*)}{m}, \\
Y_n &= \frac{4}{\Omega} \sum_{m \neq -n/2} \frac{g_{n+m} (g_m)^*}{2m + n}. \quad (\text{B3})
\end{aligned}$$

The calculation of Sect. A2 can be used to argue that the above expansion is systematic in Ω^{-1} : When the RG flow equations are truncated to a given order in $\mu_{n \neq 0}$, then the obtained equations contain all the terms of the same order (and smaller) in Ω^{-1} . This is most readily seen from Eq. (A12), where $\mu_{n \neq 0}$ only appears in the argument of the Bessel functions, and is divided by Ω . Expanding this equation in powers of $\mu_{n \neq 0}$ is actually an expansion in powers of $\mu_{n \neq 0}/\Omega$. Additionally, Ω appears in the poles of $G_{n; R}(\omega)$. Since these exclusively come with negative powers of Ω , they can not lower the order in Ω^{-1} . When the RG flow equations are truncated at a given order in $\mu_{n \neq 0}/\Omega$, then the poles only produce sub-leading (in Ω^{-1}) contributions. Both types of terms are visible in Eqs. (B2): $X_n \sim \mu/\Omega$ comes from the argument of a Bessel function and $Y_n \sim g^2/\Omega$ is the $\mathcal{O}(\Omega^{-1})$ (sub-leading) correction of a term of order zero in $\mu_{n \neq 0}/\Omega$.

In summary, the above equations are obtained through a double perturbative expansion. Eqs. (B1) are controlled for a weak coupling. They are systematic to order one in the $\epsilon = 4 - d$ expansion, as in a standard ϕ^4 analysis. Eqs. (B2) are the result of a further expansion in powers of Ω^{-1} and are systematic to order 1 as well. Our result are therefore systematic to $\mathcal{O}(\epsilon) \times \mathcal{O}(\Omega^{-1})$.

1. Monochromatic drive

Here we show that within our mesoscopic model,

$$\begin{aligned}
\mu &= \mu_0 + \mu_1 e^{i\Omega t} + \mu_{-1} e^{-i\Omega t}, \\
g &= g_0 + g_1 e^{i\Omega t} + g_{-1} e^{-i\Omega t}, \quad (\text{B4})
\end{aligned}$$

the RG flow equations can be greatly simplified because the drive is monochromatic. Specifically, we can focus on

the $n = 0$ sector

$$\begin{aligned} k\partial_k\mu_0 &= -\frac{S_d k^d \gamma}{|\text{Im}(M_0)|} (g_0 + iX_0), \\ k\partial_k g_0 &= \frac{S_d k^d \gamma}{|\text{Im}(M_0)|} \\ &\times \left\{ \left[\frac{g_0}{2M_0} + \frac{g_0 - (g_0)^*}{i\text{Im}(M_0)} \right] (g_0 + iX_0) + Y_0 \right\}, \end{aligned} \quad (\text{B5})$$

which will lead to a closed set of equations. We remark in passing that the first equation can be derived from Eq. (7) of the main text with $X_0 = x$. To order Ω^{-1} , the flow of X_0 and Y_0 is given by

$$\begin{aligned} k\partial_k X_0 &= -\frac{iS_d k^d \gamma}{2|\text{Im}(M_0)|} \left\{ Y_0 \right. \\ &\left. + \frac{1}{\Omega} \sum_{m \neq 0} \frac{(\mu_{-2m} - \mu_{2m}^*) g_m}{m} \left[\frac{g_m}{2M_0} + \frac{g_m - (g_{-m})^*}{i\text{Im}(M_0)} \right] \right\}, \\ k\partial_k Y_0 &= \frac{1}{\Omega} \frac{S_d k^d \gamma}{|\text{Im}(M_0)|} \\ &\times \sum_{m \neq 0} \frac{g_{2m}^* g_m}{m} \left[\frac{g_m}{2M_0} + \frac{g_m - g_{-m}^*}{i\text{Im}(M_0)} \right] + \text{c.c.} \end{aligned} \quad (\text{B6})$$

In the case of a monochromatic drive the last terms in Eq. (B6) can be neglected (then $k\partial_k Y_0 = 0$ and $k\partial_k X_0 \sim Y_0$) because they contain Fourier modes with $|n| \geq 2$. Indeed, the solution of the RG flow equations take the form $\mu_n(k) = \mu_n(\Lambda) + \int_k^\Lambda I(k') dk'$ (and similarly for g_n). $I(k)$ represents the loop contributions. When $\mu_n(\Lambda) = 0$ (as is the case for $|n| \geq 2$ and a monochromatic drive), then $\mu_n(k)$ is proportional to $I(k')$. The magnitude of the flow of X_0 and Y_0 is estimated by estimating g_{2m} to $\mathcal{O}(\Omega^0)$ and inserting it on the right-hand-side of Eq. (B6). Eq. (B2) provides $g_{2m} \sim g_m^2$ and $\mu_{2m} \sim g_{2m} \sim g_m^2$. Then we conclude that

$$\begin{aligned} k\partial_k Y_0 &\sim \Omega^{-1} g_1^3, \\ k\partial_k X_0 &= -\frac{iS_d k^d \gamma}{|\text{Im}(M_0)|} \frac{Y_0}{2} + \mathcal{O}(\Omega^{-1} g_1^4). \end{aligned} \quad (\text{B7})$$

Neglecting the terms that are not $\mathcal{O}(\Omega^{-1})$ and 1-loop (ϵ expansion) produces a closed set of equations

$$\begin{aligned} k\partial_k\mu_0 &= -\frac{S_d k^d \gamma}{|\text{Im}(M_0)|} (g_0 + iX_0), \\ k\partial_k g_0 &= \frac{S_d k^d \gamma}{|\text{Im}(M_0)|} \\ &\times \left\{ \left[\frac{g_0}{2M_0} + \frac{g_0 - (g_0)^*}{i\text{Im}(M_0)} \right] (g_0 + iX_0) + Y_0 \right\}, \\ k\partial_k Y_0 &= 0, \\ k\partial_k X_0 &= -\frac{iS_d k^d \gamma}{|\text{Im}(M_0)|} \frac{Y_0}{2}. \end{aligned} \quad (\text{B8})$$

2. Imaginary couplings

Eq. (B8) can be further simplified in the case of purely imaginary couplings. When the couplings can be written as $K = iK'$, $\mu(t) = i\mu'(t)$ and $g(t) = ig'(t)$ with K' , μ' and g' real, the Fourier modes satisfy

$$\mu_{-n} = -\mu_n^*, \quad g_{-n} = -g_n^*. \quad (\text{B9})$$

Inserting this in Eq. (B3) provides $Y_0 = 0$ and

$$X_0 = \frac{4}{\Omega} \sum_{m=1}^{\infty} \frac{\text{Im}(g_m^* \mu_m)}{m}, \quad (\text{B10})$$

which is a real number. The drive parameter x is defined as the real part of X_0 , and both are equal when the couplings are purely imaginary. The flow equations of the main text are written in terms of the imaginary couplings. Inserting $\mu'_0 = -i\mu_0$, $g'_0 = -ig_0$ and $K' = -iK$ into Eq. (B5) with $Y_0 = 0$ and $X_0 = \sum_m \tilde{g}_m$ and rescaling μ'_0 and g'_0 as μ_0 and g_0 [see Eq. (8) of the main text] provides Eqs. (9) and (10) of the main text (with the primes dropped).

We have checked from Eq. (B2) that, in the case of purely imaginary couplings, no real parts are generated. We can safely assume that when μ and g contain no real parts, they remain imaginary at all scales. This was already observed in [60] for time-independent couplings and is related to an additional symmetry that emerges for imaginary couplings.

Appendix C: Equilibrium symmetry

The presence of thermal equilibrium can be framed in terms of a microscopic symmetry of the dynamic action [62, 73]. In this section, we define the corresponding field transformation and (along the lines of [73]) discuss the conditions under which it is a symmetry of our system (i.e. when the dynamical action describes a thermally equilibrated system). It is instructive to consider a more general action

$$S = \int_{t,\mathbf{x}} \tilde{\phi}^* [Z^* i \partial_t \phi - \mathcal{K}(|\phi|, t) \phi] + \text{c.c.} + i\gamma |\tilde{\phi}|^2.$$

In principle, all the parameters in the above action are complex periodic functions of time. The interaction as well as the kinetic term are bundled in the operator $\mathcal{K}(|\phi|, t) = K \nabla^2 - \mu - g |\phi|^2$. Then we define the field transformation

$$\begin{pmatrix} \phi(t) \\ \tilde{\phi}(t) \\ \phi^*(t) \\ \tilde{\phi}^*(t) \end{pmatrix} \rightarrow \begin{pmatrix} \phi^*(-t) \\ \frac{r-i}{r+i} \tilde{\phi}^*(-t) + \frac{r-i}{\text{Re}(Z) - r\text{Im}(Z)} \frac{i}{2T} \partial_t \phi^*(-t) \\ \phi(-t) \\ \frac{r+i}{r-i} \tilde{\phi}(-t) + \frac{r+i}{\text{Re}(Z) - r\text{Im}(Z)} \frac{i}{2T} \partial_t \phi(-t) \end{pmatrix}, \quad (\text{C1})$$

with two (yet unspecified) parameters, r and T . This transformation is called 'equilibrium symmetry' because,

if it is possible to find values of r and T such that the above transformation is a symmetry of the action, then it can be shown [63, 64] that the system obeys fluctuation-dissipation relations with a temperature given by T .

We find that our driven system is at equilibrium when:

- (i) All the time-dependent couplings are even in t (up to a global time shift).
- (ii) There is a single (possibly time-dependent) real number $r(t)$ such that

$$\text{Re}(\mathcal{K}) = -r\text{Im}(\mathcal{K}). \quad (\text{C2})$$

This is a generalization of the requirement (found in [73]) that all the couplings lay on the same ray of the complex.

- (iii) The time-dependence of Z , γ and r are such that the temperature

$$T = \frac{(1+r^2)\tilde{\gamma}}{4[\text{Re}(Z) - r\text{Im}(Z)]}, \quad (\text{C3})$$

with $\tilde{\gamma} = \gamma/[\text{Re}(Z) - r\text{Im}(Z)]$, does not depend on time. This relation also defines T .

- (iv) \mathcal{K} satisfies

$$\frac{\partial}{\partial t} \left[\frac{1}{\tilde{\gamma}} \text{Im}[\mathcal{K}(|\phi|, t)] \right] = 0. \quad (\text{C4})$$

The time derivative does not hit the field in the above equation. This equation must be valid for all values of ϕ . It implies that there exists a time-independent operator $\mathcal{K}(|\phi|)$ such that

$$\mathcal{K}(|\phi|, t) = \tilde{\gamma} \mathcal{K}(|\phi|). \quad (\text{C5})$$

I.e. the time-dependent couplings oscillate in phase with each other.

Appendix D: Physical interpretation of x

In this section we show how the value of x Eqs. (B10) and (D2) can be related to the phases of μ_1 and g_1 . Moreover, we argue that x being identically zero can only happen at equilibrium. We focus on a monochromatic drive and purely imaginary $\mu(t)$ and $g(t)$,

$$\begin{aligned} \mu_1 &= |\mu_1|e^{i\theta_\mu}, & \mu_{-1} &= -|\mu_1|e^{-i\theta_\mu}, \\ g_1 &= |g_1|e^{i\theta_g}, & g_{-1} &= -|g_1|e^{-i\theta_g}. \end{aligned} \quad (\text{D1})$$

We start by giving a meaning to the phases of the couplings, by inserting them back into Eq. (2) of the main text,

$$\begin{aligned} \mu - \mu_0 &= \mu_1 e^{i\Omega t} - \mu_1^* e^{-i\Omega t} = 2i|\mu_1| \sin(\Omega t + \theta_\mu), \\ g - g_0 &= g_1 e^{i\Omega t} - g_1^* e^{-i\Omega t} = 2i|g_1| \sin(\Omega t + \theta_g). \end{aligned}$$

The phases of the drive couplings are phases in the time dependence of μ and g .

Inserting $\mu_1 = |\mu_1|e^{i\theta_\mu}$ and $g_1 = |g_1|e^{i\theta_g}$ into Eq. (B10) provides,

$$X_0 = 4 \frac{|\mu_1||g_1| \sin(\theta_\mu - \theta_g)}{\Omega}, \quad X_0 = \text{Re}(X_0) \equiv x. \quad (\text{D2})$$

This shows that the relative phase of μ and g plays an important role. Indeed, x can be made to vanish when μ and g are proportional to each other. On the other hand, $|x|$ is amplified when one of the couplings is lagging behind the other by a quarter of the drive period.

The present calculation may suggest that our effect is absent in a driven system when either μ_1 or g_1 is zero, or when $\theta_g = \theta_\mu$. This is however only true at $\mathcal{O}(\Omega^{-1})$. If $x = 0$ in a driven microscopic model, a non-vanishing value of x will inevitably build up under renormalization, however, only at $\mathcal{O}(\Omega^{-2})$. This is inferred from the analysis of Sect. C, which shows that x vanishes identically only when the microscopic couplings are just right for Eq. (C1) to be a symmetry of the dynamical action. This corresponds to an unnatural fine tuning of the parameters of the model.

The case of couplings with a real time-dependent part, which arises naturally when the underlying system Hamiltonian is time-dependent but the couplings to the bath are not, falls in the above category as well. Although, at a first glance, it looks like $\hat{x} = 0$, a non vanishing \hat{x} is generated by the RG.

Appendix E: Far-from-equilibrium fixed point

In the present work we find that the inclusion of a periodic drive produces an additional relevant coupling which ultimately leads to a runaway flow. This implies that criticality is only visible if the drive parameter is tuned to zero $\hat{x} = 0$. It is however possible that another attractive fixed point lies beyond the reach of our approximations. Then the system would be critical for a finite \hat{x} .

Although we can not exclude this eventuality, we find that if such a fixed point exists, then its coordinates (g^* , μ^* , x^* , etc.) must lie far away from the WF fixed point that we study since they must be proportional to a positive power of Ω . Then even though the large-scale physics would indeed be controlled by this fixed point, this would happen at very large scales since the fixed point would only be reached when $k \sim \Omega^{-1/2}$. In a system with a finite size, the phase transition would effectively remain first order for Ω large enough.

Appendix F: Analysis of the RG fixed point

In this section we give explicit expressions for the eigenvectors of the stability matrix at the WF fixed point, which emerges when $\hat{x} = 0$ in Eqs. (9) and

(10) of the main text (the canonical rescaling is $\hat{x} = k^{d-4}\gamma x/[4\text{Im}(K)^2]$).

To order $\epsilon = 4 - d$, the fixed point coordinates are

$$\vec{g}^* = \begin{pmatrix} \mu^* \\ g^* \\ x^* \end{pmatrix} \cong \begin{pmatrix} -\epsilon/5 \\ 4\pi^2\epsilon/5 \\ 0 \end{pmatrix}. \quad (\text{F1})$$

The stability matrix is then obtained by computing the Jacobian matrix of the right-hand-side of the RG flow equations and evaluating it at the WF fixed point. We find

$$M = \begin{pmatrix} -2 + \frac{2\epsilon}{5} & -\frac{4S_d}{5}(5 + \epsilon) & -\frac{4S_d}{5}(5 + \epsilon) \\ -\frac{\epsilon^2}{S_d(5+\epsilon)} & \epsilon & \epsilon \\ 0 & 0 & -\epsilon \end{pmatrix}.$$

The eigenvalues and eigenvectors of M are defined by

$$M\vec{v}_1 = -\frac{1}{\nu}\vec{v}_1, \quad M\vec{v}_2 = \epsilon\vec{v}_2, \quad M\vec{v}_3 = -\frac{1}{\nu_d}\vec{v}_3, \quad (\text{F2})$$

with $1/\nu \cong 2 - 2\epsilon/5$ and $1/\nu_d = \epsilon$, and [to $\mathcal{O}(\epsilon)$] the eigenvectors are

$$\vec{v}_1 = \begin{pmatrix} \frac{5}{4\pi^2\epsilon} + \frac{3+2P}{4\pi^2} + \frac{\epsilon}{4} \left(\frac{11+2P(P+3)}{5\pi^2} - \frac{5}{48} \right) \\ \epsilon \\ 0 \end{pmatrix},$$

$$\vec{v}_2 = \begin{pmatrix} -\frac{1}{4\pi^2} - \frac{P\epsilon}{10\pi^2} \\ 1 \\ 0 \end{pmatrix}, \quad \vec{v}_3 = \begin{pmatrix} -\frac{1}{8\pi^2} - \frac{(P+2)\epsilon}{20\pi^2} \\ -\frac{1}{2} - \frac{\epsilon}{10} \\ 1 \end{pmatrix},$$

with $P = [4 - 5(\gamma - \log(4\pi))]/4 \cong 3.442$, and $\gamma \cong 0.577$ is Euler's constant.

Writing $(\delta\mu, \delta g, \hat{x})$ as a linear combination of \vec{v}_i and expanding the result to linear order in ϵ provides

$$(\delta\mu, \delta g, \hat{x}) = \frac{\epsilon}{5} (\delta g + 4\pi^2\delta\mu + \hat{x}) \vec{v}_1 + \left[\delta g + \frac{\hat{x}}{2} \left(1 + \frac{\epsilon}{5} \right) \right] \vec{v}_2 + \hat{x} \vec{v}_3. \quad (\text{F3})$$

-
- [1] A. Eckardt, *Rev. Mod. Phys.* **89**, 011004 (2017), [arXiv:1606.08041 \[cond-mat.quant-gas\]](#).
- [2] R. Moessner and S. L. Sondhi, *Nat. Phys.* **13**, 424 (2017), [arXiv:1701.08056 \[cond-mat.dis-nn\]](#).
- [3] J. Struck, M. Weinberg, C. Ölschläger, P. Windpassinger, J. Simonet, K. Sengstock, R. Hoppner, P. Hauke, A. Eckardt, M. Lewenstein, and L. Mathey, *Nat Phys* **9**, 738 (2013), [arXiv:1304.5520 \[cond-mat.quant-gas\]](#).
- [4] N. Goldman and J. Dalibard, *Phys. Rev. X* **4**, 031027 (2014), [arXiv:1404.4373 \[cond-mat.quant-gas\]](#).
- [5] S. Choi, J. Choi, R. Landig, G. Kucsko, H. Zhou, J. Isoya, F. Jelezko, S. Onoda, H. Sumiya, V. Khemani, C. von Keyserlingk, N. Y. Yao, E. Demler, and M. D. Lukin, *Nature* **543**, 221 (2017), [arXiv:1610.08057 \[quant-ph\]](#).
- [6] A. Lerose, J. Marino, A. Gambassi, and A. Silva, [arXiv:1803.04490 \[cond-mat.stat-mech\]](#).
- [7] J. Zhang, P. W. Hess, A. Kyprianidis, P. Becker, A. Lee, J. Smith, G. Pagano, I.-D. Potirniche, A. C. Potter, A. Vishwanath, N. Y. Yao, and C. Monroe, *Nature* **543**, 217 (2017), [arXiv:1609.08684 \[quant-ph\]](#).
- [8] A. Lazarides, A. Das, and R. Moessner, *Phys. Rev. E* **90**, 012110 (2014), [arXiv:1403.2946 \[cond-mat.stat-mech\]](#).
- [9] L. D'Alessio and M. Rigol, *Phys. Rev. X* **4**, 041048 (2014), [arXiv:1402.5141 \[cond-mat.stat-mech\]](#).
- [10] M. Genske and A. Rosch, *Phys. Rev. A* **92**, 062108 (2015), [arXiv:1508.04551 \[cond-mat.quant-gas\]](#).
- [11] T. Shirai, T. Mori, and S. Miyashita, *Phys. Rev. E* **91**, 030101 (2015), [arXiv:1410.0464 \[cond-mat.stat-mech\]](#).
- [12] V. Khemani, A. Lazarides, R. Moessner, and S. L. Sondhi, *Phys. Rev. Lett.* **116**, 250401 (2016), [arXiv:1508.03344 \[cond-mat.dis-nn\]](#).
- [13] T. Shirai, T. Mori, and S. Miyashita, [arXiv:1801.02838 \[cond-mat.stat-mech\]](#).
- [14] T. Kitagawa, E. Berg, M. Rudner, and E. Demler, *Phys. Rev. B* **82**, 235114 (2010), [arXiv:1010.6126 \[cond-mat.mes-hall\]](#).
- [15] N. H. Lindner, G. Refael, and V. Galitski, *Nat. Phys.* **7**, 490 (2011), [arXiv:1008.1792 \[cond-mat.mtrl-sci\]](#).
- [16] C. Jérôme, D. Balázs, S. Ferenc, and M. Roderich, *Phys. Status Solidi* **7**, 101, [arXiv:1211.5623 \[cond-mat.mes-hall\]](#).
- [17] M. S. Rudner, N. H. Lindner, E. Berg, and M. Levin, *Phys. Rev. X* **3**, 031005 (2013), [arXiv:1212.3324 \[cond-mat.mes-hall\]](#).
- [18] T. Karzig, C.-E. Bardyn, N. H. Lindner, and G. Refael, *Phys. Rev. X* **5**, 031001 (2015), [arXiv:1406.4156 \[cond-mat.quant-gas\]](#).
- [19] L. D'Alessio and A. Polkovnikov, *Ann. Phys.* **333**, 19 (2013), [arXiv:1210.2791 \[cond-mat.stat-mech\]](#).
- [20] A. Lazarides, A. Das, and R. Moessner, *Phys. Rev. Lett.* **115**, 030402 (2015), [arXiv:1410.3455 \[cond-mat.stat-mech\]](#).
- [21] P. Ponte, A. Chandran, Z. Papić, and D. A. Abanin, *Ann. Phys.* **353**, 196 (2015), [arXiv:1403.6480 \[cond-mat.dis-nn\]](#).
- [22] K. I. Seetharam, C.-E. Bardyn, N. H. Lindner, M. S. Rudner, and G. Refael, *Phys. Rev. X* **5**, 041050 (2015), [arXiv:1502.02664 \[cond-mat.mes-hall\]](#).
- [23] M. Bukov, M. Heyl, D. A. Huse, and A. Polkovnikov, *Phys. Rev. B* **93**, 155132 (2016), [arXiv:1512.02119 \[cond-mat.quant-gas\]](#).
- [24] S. A. Weidinger and M. Knap, *Sci. Rep.* **7**, 45382 (2017), [arXiv:1609.09089 \[cond-mat.quant-gas\]](#).
- [25] E. Kandelaki and M. S. Rudner, [arXiv:1709.04448 \[cond-mat.mes-hall\]](#).
- [26] M. Bukov, S. Gopalakrishnan, M. Knap, and E. Demler, *Phys. Rev. Lett.* **115**, 205301 (2015), [arXiv:1507.01946 \[cond-mat.quant-gas\]](#).
- [27] M. Knap, M. Babadi, G. Refael, I. Martin, and E. Demler, *Phys. Rev. B* **94**, 214504 (2016), [arXiv:1511.07874 \[cond-mat.supr-con\]](#).
- [28] M. Babadi, M. Knap, I. Martin, G. Refael, and E. Demler, *Phys. Rev. B* **96**, 014512 (2017), [arXiv:1702.02531 \[cond-mat.supr-con\]](#).

- [29] Y. Murakami, N. Tsuji, M. Eckstein, and P. Werner, *Phys. Rev. B* **96**, 045125 (2017), arXiv:1702.02942 [cond-mat.supr-con].
- [30] K. I. Seetharam, C.-E. Bardyn, N. H. Lindner, M. S. Rudner, and G. Refael, arXiv:1806.10620 [cond-mat.mes-hall].
- [31] X. Xu, M. Gullans, and J. M. Taylor, *Phys. Rev. A* **91**, 013818 (2015), arXiv:1404.3726 [quant-ph].
- [32] R. Chitra and O. Zilberberg, *Phys. Rev. A* **92**, 023815 (2015), arXiv:1501.07098 [cond-mat.quant-gas].
- [33] M.-A. Lemonde, N. Didier, and A. A. Clerk, *Nat. Commun.* **7**, 11338 (2016), arXiv:1509.09238 [quant-ph].
- [34] J. Li, A. K. Harter, J. Liu, L. de Melo, Y. N. Joglekar, and L. Luo, arXiv:1608.05061 [cond-mat.quant-gas].
- [35] Z. Gong, R. Hamazaki, and M. Ueda, *Phys. Rev. Lett.* **120**, 040404 (2018), arXiv:1708.01472 [cond-mat.stat-mech].
- [36] P. Hänggi and F. Marchesoni, *Rev. Mod. Phys.* **81**, 387 (2009), arXiv:0807.1283 [cond-mat.stat-mech].
- [37] T. Salger, S. Kling, S. Denisov, A. V. Ponomarev, P. Hänggi, and M. Weitz, *Phys. Rev. Lett.* **110**, 135302 (2013), arXiv:1202.5174 [cond-mat.quant-gas].
- [38] S. Denisov, S. Flach, and P. Hänggi, *Phys. Rep.* **538**, 77 (2014), arXiv:1311.1086 [cond-mat.mes-hall].
- [39] J. Stehlik, Y.-Y. Liu, C. Eichler, T. R. Hartke, X. Mi, M. J. Gullans, J. M. Taylor, and J. R. Petta, *Phys. Rev. X* **6**, 041027 (2016), arXiv:1607.08229 [cond-mat.mes-hall].
- [40] A. Lazarides and R. Moessner, *Phys. Rev. B* **95**, 195135 (2017), arXiv:1703.02547 [cond-mat.stat-mech].
- [41] K. Iwahori and N. Kawakami, *Phys. Rev. A* **95**, 043621 (2017), arXiv:1702.03506 [cond-mat.stat-mech].
- [42] S. De Sarkar, R. Sensarma, and K. Sengupta, *J. Phys. Condens. Matter* **26**, 325602 (2014), arXiv:1308.4689 [cond-mat.str-el].
- [43] G. Nikoghosyan, R. Nigmatullin, and M. B. Plenio, *Phys. Rev. Lett.* **116**, 080601 (2016), arXiv:1311.1543 [cond-mat.stat-mech].
- [44] B. Feng, S. Yin, and F. Zhong, *Phys. Rev. B* **94**, 144103 (2016), arXiv:1604.04345 [cond-mat.stat-mech].
- [45] G. Korniss, C. J. White, P. A. Rikvold, and M. A. Novotny, *Phys. Rev. E* **63**, 016120 (2000), cond-mat/0008155.
- [46] H. Fujisaka, H. Tutu, and P. A. Rikvold, *Phys. Rev. E* **63**, 036109 (2001), cond-mat/0009284.
- [47] G. M. Buendía and P. A. Rikvold, *Phys. Rev. E* **78**, 051108 (2008), arXiv:0809.0523 [cond-mat.stat-mech].
- [48] S. Coleman and E. Weinberg, *Phys. Rev. D* **7**, 1888 (1973).
- [49] B. I. Halperin, T. C. Lubensky, and S.-K. Ma, *Phys. Rev. Lett.* **32**, 292 (1974).
- [50] M. E. Fisher and D. R. Nelson, *Phys. Rev. Lett.* **32**, 1350 (1974).
- [51] D. R. Nelson, J. M. Kosterlitz, and M. E. Fisher, *Phys. Rev. Lett.* **33**, 813 (1974).
- [52] G. R. Golner, *Phys. Rev. B* **8**, 3419 (1973).
- [53] F. Y. Wu, *Rev. Mod. Phys.* **54**, 235 (1982).
- [54] J. Manuel Carmona, A. Pelissetto, and E. Vicari, *Phys. Rev. B* **61**, 15136 (2000), cond-mat/9912115.
- [55] A. Aharony, *J. Stat. Phys.* **110**, 659 (2003), cond-mat/0201576.
- [56] I. Carusotto and C. Ciuti, *Rev. Mod. Phys.* **85**, 299 (2013), arXiv:1205.6500 [cond-mat.quant-gas].
- [57] L. M. Sieberer, M. Buchhold, and S. Diehl, *Rep. Prog. Phys.* **79**, 096001 (2016), arXiv:1512.00637 [cond-mat.quant-gas].
- [58] A. J. Daley, *Adv. Phys.* **63**, 77 (2014), arXiv:1405.6694 [quant-ph].
- [59] U. C. Täuber and S. Diehl, *Phys. Rev. X* **4**, 021010 (2014), arXiv:1312.5182 [cond-mat.stat-mech].
- [60] L. M. Sieberer, S. D. Huber, E. Altman, and S. Diehl, *Phys. Rev. Lett.* **110**, 195301 (2013), arXiv:1301.5854 [cond-mat.quant-gas].
- [61] A. Kamenev, *Field theory of non-equilibrium systems* (Cambridge University Press, 2011).
- [62] U. Täuber, *Critical Dynamics: A Field Theory Approach to Equilibrium and Non-Equilibrium Scaling Behavior* (Cambridge University Press, 2014).
- [63] L. M. Sieberer, A. Chiocchetta, A. Gambassi, U. C. Täuber, and S. Diehl, *Phys. Rev. B* **92**, 134307 (2015), arXiv:1505.00912 [cond-mat.stat-mech].
- [64] C. Aron, G. Biroli, and L. F. Cugliandolo, *SciPost Phys.* **4**, 008 (2018), arXiv:1705.10800 [cond-mat.stat-mech].
- [65] L. Arrachea, *Phys. Rev. B* **72**, 125349 (2005), cond-mat/0505153.
- [66] B. H. Wu and J. C. Cao, *J. Phys. Condens. Matter* **20**, 085224 (2008).
- [67] G. Stefanucci, S. Kurth, A. Rubio, and E. K. U. Gross, *Phys. Rev. B* **77**, 075339 (2008), cond-mat/0701279.
- [68] N. Tsuji, T. Oka, and H. Aoki, *Phys. Rev. B* **78**, 235124 (2008), arXiv:0808.0379 [cond-mat.str-el].
- [69] The phase with broken $U(1)$ symmetry however exhibits gapless Goldstone modes. In $d > 2$ dimensions, the associated IR fluctuations are phase space suppressed and do not destroy the ordered phase of an undriven system. Because the divergences emerging from the drive are copies of the single undriven divergence, we do not expect the presence of a drive to alter this behavior qualitatively.
- [70] T. W. B. Kibble, *J. Phys. A: Math. Gen.* **9**, 1387 (1976).
- [71] W. H. Zurek, *Nature* **317**, 505 (1985).
- [72] O. Howell, P. Weinberg, D. Sels, A. Polkovnikov, and M. Bukov, arXiv:1802.04910 [cond-mat.stat-mech].
- [73] L. M. Sieberer, S. D. Huber, E. Altman, and S. Diehl, *Phys. Rev. B* **89**, 134310 (2014), arXiv:1309.7027 [cond-mat.quant-gas].